https://doi.org/10.5194/egusphere-2026-2202
Preprint. Discussion started: 27 May 2026

Lagged Responses of Seasonally Frozen Ground on the Qinghai-Tibet Plateau to Extreme Heat Events

Ting Zhang[1], Tingbin Zhang[1,2], Xianglong Ma[3], Guihau Yi[3], Xianhang Zhou[1]

[1]College of Earth and Planet Science, Chengdu University of Technology, Chengdu 610059, China
[2]Middle Yarlung Zangbo River Natural Resources Observation and Research Station of Xizang Autonomous Region, Lhasa, 850013, China
[3]College of Geography and Planning, Chengdu University of Technology, Chengdu 610059, China

Correspondence to: Tingbin Zhang (zhangtb@cdut.edu.cn)

https://doi.org/10.5194/egusphere-2026-2202
Preprint. Discussion started: 27 May 2026

Abstract. Extreme heat events can induce delayed responses in seasonally frozen ground (SFG) by altering soil heat storage and release processes, yet their lag characteristics and spatial variability remain poorly quantified. Here, we develop a distributed lag nonlinear model integrated with an explainable artificial intelligence framework (DLNM-XAI) to quantify the lagged responses of SFG to extreme heat events across the Qinghai-Tibet Plateau (QTP), based on in situ observations, multi-source remote sensing, and reanalysis datasets. Results show that extreme heat significantly modifies freeze–thaw dynamics. On average, each additional extreme heat day advances the thaw end date by 3.02 days, delays the freeze onset date by 1.52 days, and reduces maximum freezing depth by approximately 1.12 cm. The response of freezing depth exhibits a clear nonlinear lag pattern, with effects emerging within 5-10 days, peaking after approximately 15-20 days, and gradually weakening thereafter. Spatially, lagged responses also show pronounced spatial heterogeneity across the QTP. Regions with deeper snow cover, higher soil moisture, and stronger surface energy exchange generally exhibit longer lag durations. These factors, including extreme heat duration, snow depth, soil moisture, and surface energy fluxes, jointly regulate soil heat transfer and energy retention, thereby modulating the timing and persistence of SFG responses. Overall, this study provides a regional-scale characterization of the delayed thermal responses of SFG to extreme heat events and improves understanding of thermal memory and land-atmosphere interactions under short-term extreme climate forcing in cold regions.

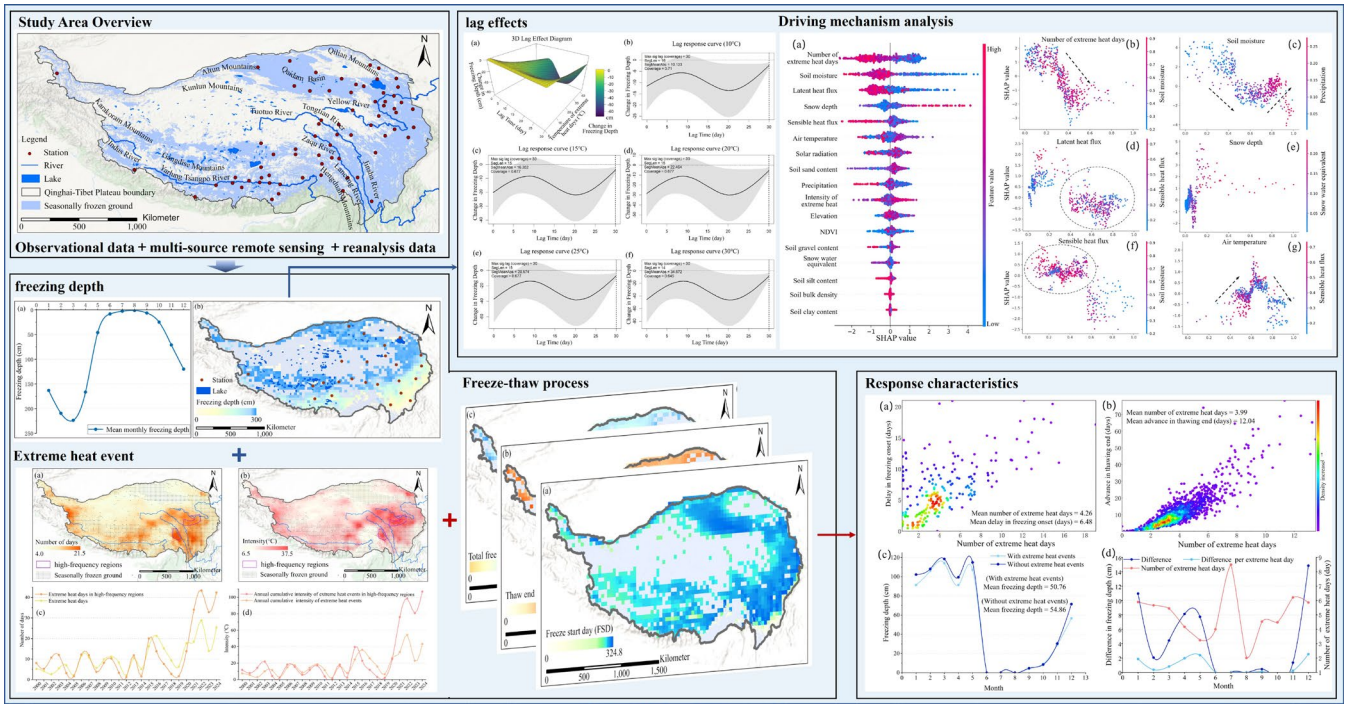

https://doi.org/10.5194/egusphere-2026-2202
Preprint. Discussion started: 27 May 2026

1 Introduction

Extreme heat events represent some of the most frequent and intense climatic anomalies under ongoing global warming (Bai et al., 2014; Banerjee et al., 2025; Horton et al., 2016). The short-term thermal perturbations not only pose direct threats to ecosystems, agriculture, and human health but also profoundly reshape land-atmosphere energy exchanges and hydrothermal cycles, thereby altering both surface and subsurface thermodynamic states (Parker et al., 2020; Teskey et al., 2015; Ye et al., 2025). Seasonally frozen ground (SFG), which is widely distributed in mid- to high-latitude and high-altitude regions, is highly sensitive to atmospheric thermal forcing because of recurrent freeze-thaw processes and subsurface heat storage. (Tao et al., 2025). Extreme heat events can disrupt the surface-subsurface energy balance by enhancing sensible heat flux, suppressing latent heat flux, and altering snow cover properties such as albedo and thickness (Song et al., 2022), which consequently may modify freeze-thaw dynamics, freezing depth, and the long-term energy budget within the active layer (Xu et al., 2025). Due to the relatively slow thermal adjustment of subsurface soils, SFG may exhibit delayed and cumulative responses to short-term climate extremes (Li et al., 2025). Therefore, understanding the lagged responses of SFG to extreme heat events is essential for clarifying delayed feedback in land-atmosphere energy exchange and improving land surface modeling and climate risk assessments in cold regions (Bibi et al., 2018; Stiegler et al., 2016).

As the region with the most extensive mid- to low-latitude SFG distribution, the Qinghai-Tibet Plateau (QTP) is highly sensitive to climatic perturbations (Ran et al., 2022b; Xu et al., 2025). Over the past two decades, the plateau has experienced a persistent rise in mean air temperature, accompanied by a pronounced increase in the frequency and intensity of extreme heat events (Zhang et al., 2023), with local heatwaves exhibiting sustained and cumulative characteristics (Ji and Kang, 2015; Yu et al., 2021). Concurrently, multiple observational records and modeling results indicate significant changes in the freeze–thaw processes of SFG on the QTP, including reduced freezing depth, shortened freezing duration, earlier thaw onset, and delayed freezing onset (Gao et al., 2021; Wen et al., 2023). Existing studies have primarily focused on multi-year variability and emphasized the cumulative response of SFG to long-term climatic forcing (Li et al., 2023), whereas the responses of SFG to short-term extreme heat events remain insufficiently investigated. Existing borehole-based analyses indicate that intense heatwave events lead to a shallower frozen layer and delayed soil thermal responses on the QTP (Zhu et al., 2024). However, these studies are generally limited by sparse observations and insufficient regional representativeness, making it difficult to systematically characterize the temporal and spatial patterns of lagged SFG responses at the plateau scale.

To reveal the response processes of SFG to short-term thermal extremes, several key questions remain unresolved. Firstly, limited data continuity and spatial representativeness hinder the systematic characterization of plateau-wide SFG responses to extreme heat (Pascual and Johansson, 2022). It remains unclear whether SFG responses to extreme heat exhibit consistent lag structures across the QTP and how these lag characteristics vary spatially. Secondly, the nonlinear and delayed responses of freezing processes to short-term thermal extremes have not been quantitatively characterized at regional scales. Existing studies focus on thermal evolution and degradation processes under long-term climatic warming (Kang et al., 2010), while

https://doi.org/10.5194/egusphere-2026-2202
Preprint. Discussion started: 27 May 2026

few quantitatively model the nonlinear and lagged behaviors of SFG under short-duration, high-intensity heat disturbances. And previous simulations based on soil temperature profiles or energy-balance equations often assume linear heat conduction and neglect latent heat and soil-moisture coupling effects (Mihalakakou et al., 1997; Yao et al., 2011), leading to limitations in reproducing the dynamic evolution of freezing depth. Thirdly, the environmental factors controlling the spatial heterogeneity of lag duration remain insufficiently understood. Variations in snow cover, soil moisture, and surface energy exchange may jointly influence subsurface heat storage and transfer processes (Ma et al., 2022). However, the nonlinear interactions and cumulative effects among these hydrothermal processes are inherently complex and are difficult to capture using traditional statistical approaches (Staniec and Nowak, 2016), making it challenging to disentangle their relative contributions to lagged SFG responses under extreme heat conditions.

Aiming to address these issues, this study integrates observations, reanalysis datasets, and multi-source remote sensing data to investigate the lagged responses of SFG to extreme heat events across the QTP. A combined Distributed Lag Nonlinear Model and eXplainable Artificial Intelligence (DLNM-XAI) framework is then established to quantify the nonlinear lagged effects of extreme heat and to elucidate the driving mechanisms of lagged responses in SFG. Specifically, this study aims to: characterize the responses of freeze–thaw processes and maximum freezing depth to extreme heat events; quantify the temporal characteristics and spatial variability of lagged responses across the QTP; and examine the hydrothermal and surface energy factors associated with regional differences in lag duration. This study improves understanding of delayed thermal responses and land-atmosphere interactions in cold regions under short-term climate extremes.

2 Data and Methods

2.1 Data Sources

This study integrates ground-based observations, multi-source reanalysis products, and remote sensing datasets, encompassing variables covering a wide range of environmental variables such as freezing depth, meteorological conditions, soil properties, hydrological indicators, and surface energy fluxes.

Ground-observed freezing depth data were derived from Middle Yarlung Zangbo River Natural Resources Observation and Research Station (2024YJZKF002) and the Second QTP Scientific Expedition and Research Program (Grant No. 2019QZKK0307). Observation sites are primarily distributed across the eastern and southeastern mid- to low-elevation regions of the plateau, whereas monitoring data in the central and western sectors are relatively sparse (Fig.1). Monthly maximum freezing-depth data were used both to quantify the response characteristics of freezing depth to extreme heat events and to validate the accuracy of simulated freezing-depth data, ensuring the reliability of subsequent lag-effect analyses.

https://doi.org/10.5194/egusphere-2026-2202
Preprint. Discussion started: 27 May 2026

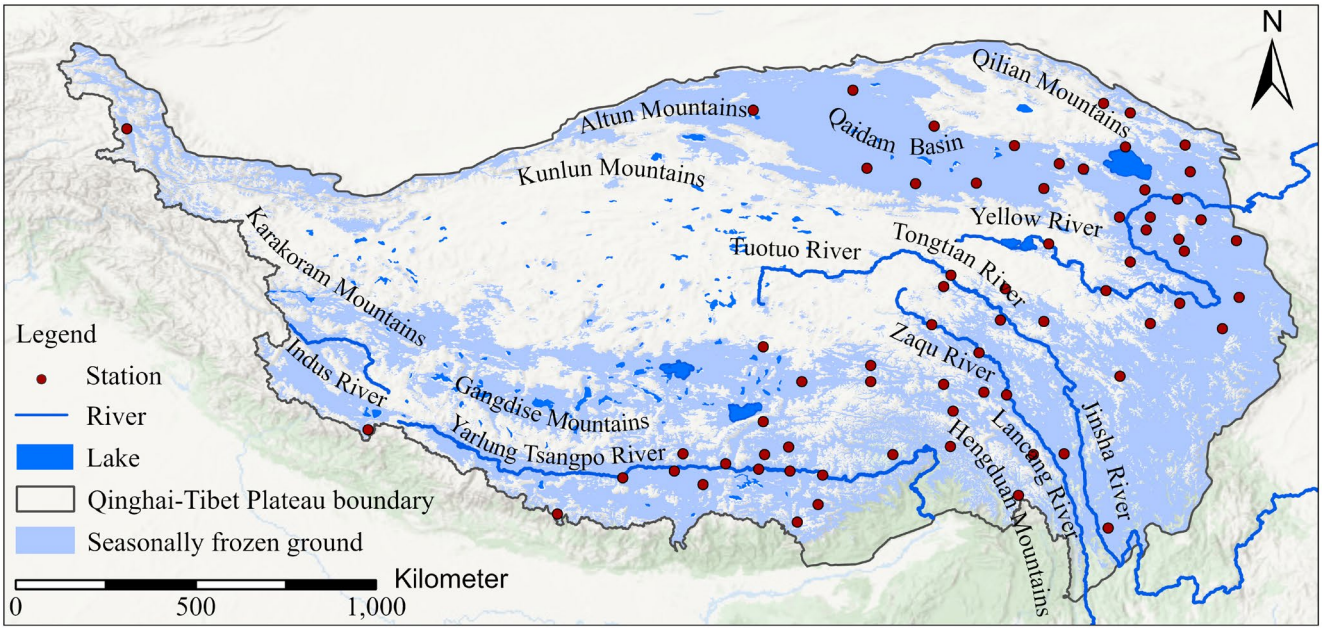

Figure 1: Spatial distribution of freezing-depth observation station (the extent of seasonally frozen ground is derived from Ran et al. (2022a)

CMA-RA/Land incorporates a denser network of in situ observations over China and is optimized for the complex topography of the Tibetan Plateau and land-atmosphere interactions. It shows improved regional performance in simulating soil temperature, soil moisture, and surface energy fluxes (Liu et al., 2023). Thence, this study uses CMA-RA/Land for climate variables. Meteorological variables from ERA5-Land (Muñoz-Sabater et al., 2021). Vegetation index from NASA's MODIS NDVI product MOD13A2 (Liu et al., 2017). Soil property data were obtained from the China High-Resolution National Soil Information Grids dataset, provided by the National Earth System Science Data Center of China (Liu et al., 2022). And topographic information from NASA's SRTMGL1 v003 product (Chymyrov, 2021). Detailed data sources and descriptions are summarized in Table 1.

Table 1. Details of data sources

Data	environmental variables	Data source	Spatial Resolution
CMA-RA/Land	stratified soil temperature, soil moisture, snow depth, snow water equivalent, sensible heat flux, and latent heat flux	https://data.cma.cn/	34 km
ERA5-Land	air temperature, precipitation, and solar radiation	https://cds.climate.copernicus.eu/	10 km
MOD13A2	Vegetation index (NDVI)	https://lpdaac.usgs.gov/	1 km
SRTMGL1	elevation	https://developers.google.com/	30 m
Soil data	sand content, gravel content, silt content, bulk density, clay content	https://www.geodata.cn/main/	10 km

https://doi.org/10.5194/egusphere-2026-2202
Preprint. Discussion started: 27 May 2026

In this study, based on the layered soil-temperature data, the spatiotemporal distribution of freezing depth on the QTP was derived through interpolation. Air-temperature data were used to identify the timing and intensity of extreme heat events. On the temporal scale, snow depth, snow water equivalent, soil moisture, sensible and latent heat fluxes, NDVI, shortwave radiation, and precipitation were used as covariates in the lag-effect analysis. On the spatial scale, variables including soil moisture, latent and sensible heat fluxes, snow depth, solar radiation, precipitation, elevation, NDVI, snow water equivalent, and soil properties were employed to identify dominant driving mechanisms.

2.2 Methods

The research followed a four-stage technical framework (Fig.2). In the first stage, the freezing depth and freeze-thaw indicators of SFG were established. Layered soil-temperature data were interpolated to delineate the boundaries of the frozen layer, from which daily freezing depth was calculated to characterize the freeze-thaw evolution. The second stage focused on the identification and characterization of extreme heat events. Daily air-temperature data were used to detect extreme heat occurrences and to derive their annual frequency and intensity characteristics. In the third stage, freeze-thaw indicators were integrated with extreme heat event records to conduct a baseline-based anomaly analysis, thereby quantifying how seasonal frozen-ground thermal indicators respond to extreme heat exposure. Finally, the fourth stage involved a lag-effect and driving-mechanism analysis. By combining freezing-depth data with extreme heat event observations, this stage aimed to quantify the lagged response of freezing depth to extreme heat and to elucidate the spatial heterogeneity and controlling mechanisms of the lag effects.

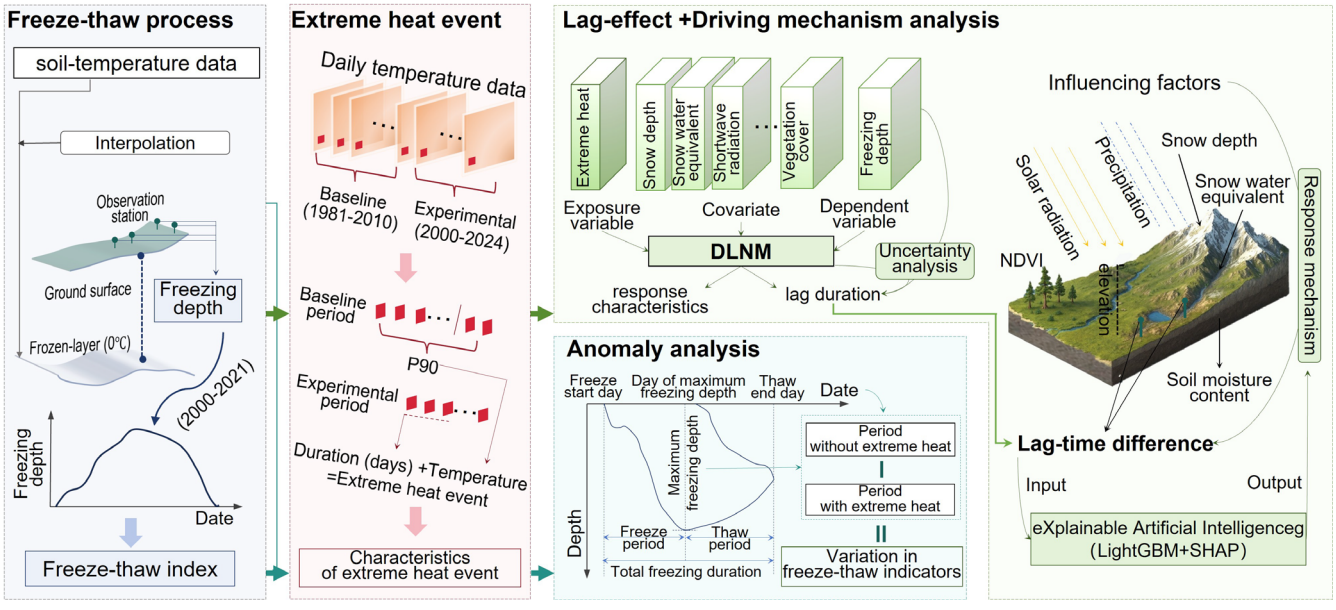

Figure 2: Technical workflow for analyzing the lagged thermal response of seasonal frozen ground to extreme heat events.

https://doi.org/10.5194/egusphere-2026-2202
Preprint. Discussion started: 27 May 2026

2.2.1 Calculation of Freeze-Thaw Indicators

Meteorological observation stations on the QTP are sparse and unevenly distributed, limiting their ability to capture regional variations in freezing depth. Furthermore, the low temporal resolution of monthly data is insufficient for daily-scale lag analyses. Therefore, this study adopts an interpolation-based approach using multilayer soil temperature profiles to identify freezing conditions within the soil column. Considering the downward freezing and complex thawing processes of SFG, a depth-corrected linear interpolation is applied to multilayer soil temperature data (0-0.1 m, 0.1-0.4 m, 0.4-1 m, and 1-2 m) to estimate the position of the 0°C isotherm along the vertical profile (Frauenfeld and Zhang, 2011). When the freezing front extended below the deepest observed layer (2.0 m), a controlled linear extrapolation was applied using the temperature gradient between the deepest available layers to estimate the lower freezing boundary.

Freezing depth is defined as the vertical distance from the ground surface to the lower freezing front identified by the 0°C isotherm. The maximum freezing depth within each month is taken as the monthly maximum freezing depth. If the estimated lower freezing front exceeds a threshold depth of 5 m, the interpolation is considered unreliable, and the corresponding daily value is discarded to avoid errors caused by excessive extrapolation.

Then, the reliability of the interpolated freezing depths was assessed by comparing them with observed freezing depth measurements using the Pearson correlation test (Van den Heuvel and Zhan, 2022). The Pearson correlation coefficient is calculated as follows:

$$r = \frac{\sum_{i=1}^{n}(x_i-\bar{x})(y_i-\bar{y})}{\sqrt{\sum_{i=1}^{n}(x_i-\bar{x})^2}\sqrt{\sum_{i=1}^{n}(y_i-\bar{y})^2}}, \quad (1)$$

Where r represents the Pearson correlation coefficient, ranging from −1 to 1; x_i and y_i are the observed values of the two variables for the $x-th$ sample; $\bar{x}$ and $\bar{y}$ denote their respective means; and n is the total number of samples.

To systematically characterize the interannual freeze-thaw dynamics of SFG, six key freeze-thaw indicators were extracted from daily freezing depth time series: freeze start day (FSD), freeze period (FPT), day of maximum freezing depth (MFD_day), thaw period (MPT), thaw end day (TMD), and total freezing duration (FDT) (Luo et al., 2020). Specifically, FSD was defined as the first day on which freezing depth exceeded 0 cm for at least three consecutive days during the freezing season, while TMD was defined as the last day with freezing depth greater than 0 cm before complete thawing. Delayed freezing onset and advanced thawing end were quantified by comparing annual FSD and TMD anomalies during extreme heat years relative to the climatological mean baseline period. MFD_day was defined as the day of the year corresponding to the annual maximum freezing depth. FPT and MPT respectively represent the durations of the freezing and thawing stages, while FDT denotes the total annual duration of frozen conditions.

Collectively, these indicators capture the formation, development, and thawing processes of SFG, maintain temporal continuity and physical consistency, and provide a robust basis for subsequent analyses of freeze-thaw dynamics and lagged responses under extreme heat events (Zhao et al., 2022).

https://doi.org/10.5194/egusphere-2026-2202
Preprint. Discussion started: 27 May 2026

2.2.2 Identification of Extreme Heat Events

The percentile threshold method is widely recognized as an effective approach for identifying extreme heat events in climate research (Sulikowska and Wypych, 2020). Unlike fixed-temperature criteria (e.g., 35 °C), the percentile-based method mitigates underestimation of extremes in cooler plateau regions and simultaneously accounts for spatial heterogeneity and temporal continuity, making it well-suited to the complex topography and pronounced climatic variability of the QTP (Brunner and Voigt, 2024; Di Napoli et al., 2019).

Using 1981-2010 as the climatological baseline, a 31-day moving window (15 days before and after each calendar day) was applied to the daily mean temperature series to calculate the 90th percentile (P90) as the daily extreme heat threshold. During the study period, an extreme heat event was defined when daily maximum temperatures exceeded the corresponding P90 for at least three consecutive days.

For each event, key characteristics, including onset and end dates, duration, and intensity, are further extracted to describe the frequency, persistence, and thermal magnitude of extreme heat events. Here, the temperature of extreme days refers to the observed daily maximum temperature during days identified as extreme heat events, and representative temperature levels (10 °C, 15 °C, 20 °C, 25 °C, and 30 °C) were selected to characterize lag-response patterns under different extreme heat conditions. Daily heat intensity was defined as the exceedance of observed temperature above the corresponding threshold, and the cumulative heat intensity of an extreme heat event was calculated as the sum of daily exceedance values during the event period. This framework effectively captures the spatiotemporal variability and evolution of extreme heat under the complex topographic conditions of the QTP (Barriopedro et al., 2023).

2.2.3 Distributed Lag Non-linear Model–Explainable Artificial Intelligence (DLNM-XAI) Model

To quantitatively identify the maximum lag time of SFG on the QTP in response to extreme heat events, and to reveal the dominant driving factors and their interactive mechanisms, this study constructs a Distributed Lag Non-linear Model-Explainable Machine Learning (DLNM-XAI) research framework. This framework jointly accounts for temporal lag effects, nonlinear responses, and multi-factor coupling characteristics (Gasparrini and Armstrong, 2013), enabling characterization of the dynamic thermal response and lagged driving mechanisms of SFG under extreme heat conditions on the QTP.

Extreme heat impacts on SFG are characterized by delayed thermal adjustments and nonlinear responses caused by subsurface heat storage and freeze-thaw processes. Traditional sinusoidal or phase-lag models generally assume stationary periodic variations with fixed lag structures, which are effective for representing seasonal cyclic changes but are less suitable for capturing event-driven, nonlinear, and temporally evolving responses to short-term thermal extremes. In contrast, the responses of freezing depth and freeze–thaw timing to extreme heat events may exhibit threshold effects, asymmetric lag durations, and cumulative thermal influences that evolve dynamically over time.

In the lag effect analysis, the Distributed Lag Nonlinear Model (DLNM) simultaneously quantifies the effects of a climatic exposure variable across both intensity and temporal dimensions (Gasparrini, 2014). The term “distributed lag” refers to the

https://doi.org/10.5194/egusphere-2026-2202
Preprint. Discussion started: 27 May 2026

influence of a single extreme heat event being distributed across multiple subsequent time periods rather than occurring at one fixed lag time. This framework, therefore, allows the cumulative effects of extreme heat to evolve dynamically over time and is well suited for investigating delayed freeze-thaw responses in SFG under short-term thermal disturbances (Gasparrini et al., 2017; Neophytou et al., 2018).

In the DLNM model, extreme heat intensity is treated as the exposure variable, and freezing depth as the response variable. Using a cross-basis function, smooth functions are fitted along both the exposure and lag dimensions, allowing the model to characterize the nonlinear effects of heatwaves on freezing depth across varying intensities and lag times. To isolate the effects of extreme heat from other environmental influences, several hydrothermal covariates potentially affecting freeze-thaw processes were included in the modeling framework, including precipitation, snow depth, soil moisture, and surface energy fluxes. These variables were incorporated as control factors to reduce confounding effects. The framework permits lagged effects to decay or accumulate nonlinearly over time, realistically reflecting the delayed response and "thermal memory" of the frozen layer. Model is expressed as:

$$Y_t = \alpha + cb\left(X_t;\beta\right) + \sum_{k=1}^{p} S\left(Z_{k,t}\right) + \varepsilon_t \quad (2)$$

$$\mathrm{cb}\left(X_t;\beta\right) = \sum_{i=1}^{I}\sum_{j=0}^{L} \beta_{ij} \mathrm{B}_i\left(X_t\right) C_j\left(l\right) \quad (3)$$

where Y_t represents the freezing depth on day t, and X_t denotes the extreme heat intensity on the same day. The term $cb\left(X_t;\beta\right)$ is the cross-basis function, while $S\left(Z_{k,t}\right)$ represents a smooth function of the $k-th$ environmental covariate at day t, used to control for potential confounding effects. Here, $Z_{k,t}$ includes hydrothermal variables potentially affecting freeze-thaw processes, including precipitation, soil moisture, snow depth, and sensible and latent heat fluxes. ε_t is an independently and identically distributed error term. $B_i\left(X_t\right)$ and $C_j\left(l\right)$ represent the basis functions for the exposure and lag dimensions, respectively; L is the maximum lag (set to 30 days in this study), and β_{ij} denotes the corresponding coefficient matrix.

The Explainable Artificial Intelligence (XAI) component was developed based on the Light Gradient Boosting Machine (LightGBM) and SHapley Additive exPlanations (SHAP) frameworks. This approach explicitly accounts for nonlinear relationships and interaction effects among variables, and quantitatively assesses the contributions and directional influences of environmental variables on variations in lag time. LightGBM is an improved algorithm derived from the Gradient Boosting Decision Tree (GBDT) framework. By adopting histogram-based split optimization and a leaf-wise tree growth strategy, LightGBM enables efficient nonlinear regression modeling (Friedman, 2001). It excels at handling high-dimensional climate datasets, automating feature selection, and providing high computational efficiency (Hajihosseinlou et al., 2023; Ke et al., 2017), and has been widely applied in climate prediction, land surface modeling, and permafrost dynamics analysis. In this study, input variables included the number of extreme heat days, soil moisture, latent heat flux, mean annual snow depth, and soil composition, while the output was the maximum lag time. Based on the LightGBM model, the SHAP method was introduced to conduct interpretability analysis (Mi et al., 2020). Grounded in game theory, SHAP

https://doi.org/10.5194/egusphere-2026-2202
Preprint. Discussion started: 27 May 2026

computes the average marginal contribution (Shapley value) of each feature across all possible combinations, quantifying both the magnitude and direction of its effect on model predictions (Van den Broeck et al., 2022). This approach not only elucidates the influence of individual factors but also reveals feature interactions and nonlinear dependencies, providing a mechanistic explanation for the spatial heterogeneity and governing processes of lagged responses.

3 Results and Analysis

3.1 Spatiotemporal Patterns of Extreme Heat Events

Since 2000, extreme heat events on the QTP have exhibited a clear trend of expansion in spatial extent, increase in frequency, and intensification in magnitude (Fig.3). Most regions of the Plateau experience at least one extreme heat event (≥ 3 days) per year on average, indicating that extreme thermal disturbances have become a persistent component of the regional climate regime.

From a spatial perspective, extreme heat events exhibit a distinct decreasing gradient from the southeast toward the northwest. Plateau's southeastern areas, including southeastern QTP, the Nujiang Valley, and southern Qinghai, experience approximately 20 hot days per year, with a cumulative intensity reaching 35 °C. In contrast, the central-northern regions, such as Qiangtang and the northern foothills of the Kunlun Mountains, experience fewer than 5 hot days per year, with a cumulative intensity of about 10 °C (Fig.3a, b). This gradient pattern is primarily controlled by topographic relief, latitudinal variation, and radiative flux, reflecting the spatial heterogeneity of surface energy input. Temporally (Fig.3c, d), both the frequency and intensity of extreme heat events increased significantly from 2000 to 2024, with a particularly sharp rise observed in recent years (2021-2024). The year 2022 marked the peak, when southeastern regions experienced more than 30 hot days, with a cumulative intensity of approximately 80 °C.

Overall, extreme heat events over the QTP show pronounced spatial contrasts, with higher occurrence and intensity in the southeastern region and much weaker signals toward the northwest, together with a clear intensification over recent decades. Within the SFG region, high-frequency regions are mainly concentrated in the Hengduan Mountains and adjacent southeastern plateau areas (Fig.3a, b), where extreme heat events occur more frequently and exhibit higher cumulative intensity than the plateau average. These patterns reflect the combined influences of regional warming, anomalous atmospheric circulation, and enhanced surface energy absorption.

https://doi.org/10.5194/egusphere-2026-2202
Preprint. Discussion started: 27 May 2026

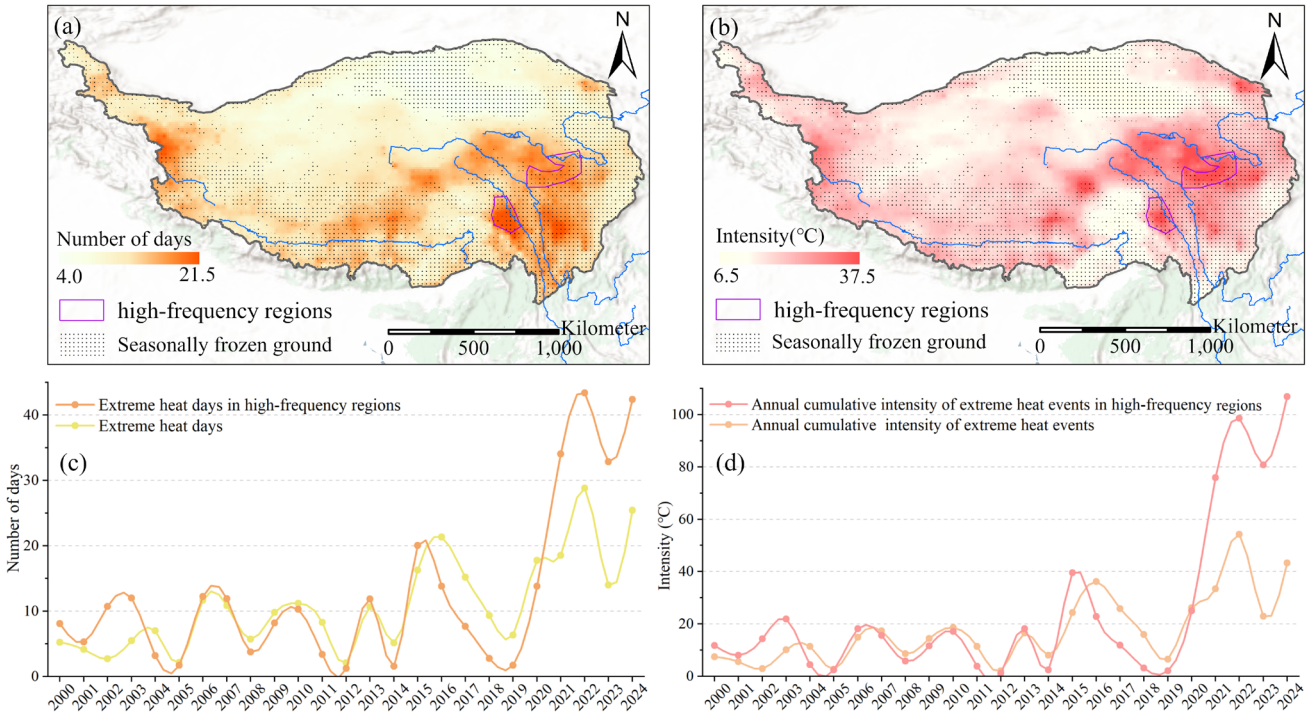

Figure 3: Spatial and temporal patterns of extreme heat events on the Qinghai-Tibet Plateau (2000-2024): (a) Annual number of extreme heat days (days yr^{-1}); (b) annual cumulative intensity of extreme heat events (°C); (c) temporal variations in annual number of extreme heat days across the QTP and high-frequency regions; (d) temporal variations in annual cumulative intensity across the QTP and high-frequency regions

3.2 Freeze-thaw processes of seasonally frozen ground

Monthly data from 69 stations covering 2000-2015 were used for Pearson correlation analysis, yielding 2702 valid observations after removing abnormal and missing records. The results show a strong positive correlation between simulated and observed monthly maximum freezing depth (R = 0.77), indicating that the interpolation scheme effectively captures the temporal evolution and spatiotemporal patterns of freezing depth. Although a systematic bias is present (Bias = 39.79 cm) and the RMSE is approximately 54.01 cm, the errors are primarily characterized by a consistent offset rather than random fluctuations (Fig. A1). This suggests that the model performs reliably in representing relative variations and overall trends. Therefore, the simulated results remain suitable for analyses focusing on trend-based lag response characteristics. It should be noted that correlations vary seasonally: during the fully thawed period (June-August), coefficients are lower than in the freezing season (October-April), with February reaching as high as 0.8. This pattern reflects freeze–thaw dynamics that predictions near zero during the fully thawed period are conservative, reducing correlation.

Based on the predicted freezing depth, the analysis shows that the freezing depth exhibits a characteristic unimodal annual pattern, rising rapidly during January and February to reach a maximum of approximately 224 cm in March. As air temperatures increase, the freezing depth gradually decreases to a minimum between June and August, before rising again

https://doi.org/10.5194/egusphere-2026-2202
Preprint. Discussion started: 27 May 2026

after September (Fig.4a). Spatially, taking March as an example, the mean frozen layer exhibits a pronounced gradient influenced by topography, elevation, air temperature gradients, and surface conditions (Fig.4b), with deeper layers concentrated in the central Plateau and shallower layers along the margins. Regions exceeding 200 cm, including the Tanggula Mountains, Kunlun Mountains, and Qiangtang Plateau, are confined to the central and northwestern Plateau, whereas freezing depths generally remain below 50 cm in the southeastern Plateau and major river valleys. These spatial patterns are generally consistent with the plateau-scale assessment of SFG dynamics reported by Ji et al. (2026)., who similarly identified deeper freezing depths in the high-elevation central and northwestern Plateau and shallower freezing in southeastern and valley regions using a sinusoidal heat-transfer model. Although differences in absolute values may arise from methodological differences, the strong agreement in regional spatial patterns suggests that the interpolation-based approach used in this study can reliably capture large-scale variations in freezing depth across the QTP.

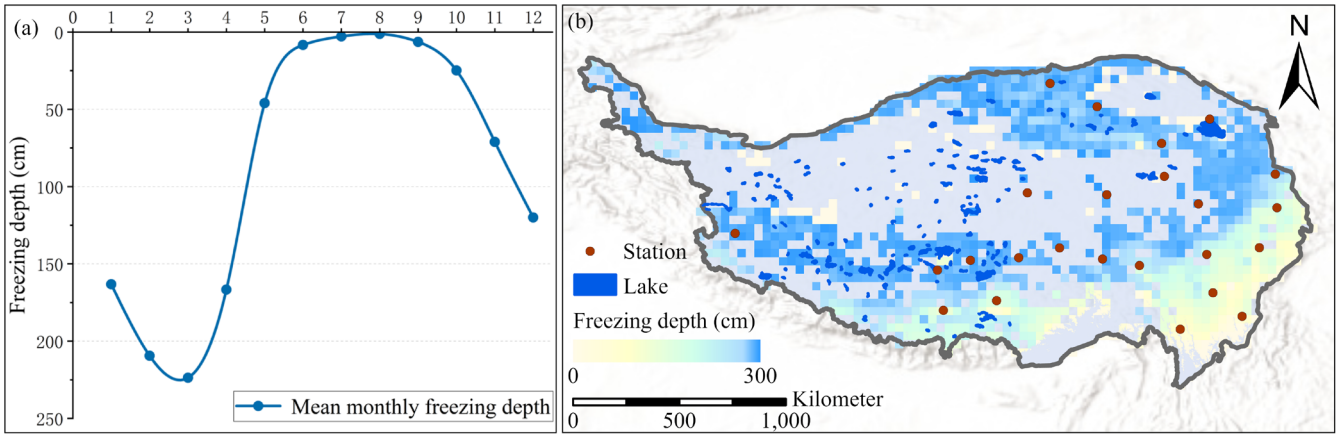

Figure 4: Freezing depth on the Qinghai-Tibet Plateau during 2000-2021: (a) Monthly mean freezing depth averaged; (b) spatial distribution of mean freezing depth in March

The freeze-thaw cycle is seasonal and periodic, with freezing in autumn-winter and thawing in spring-summer. SFG typically begins freezing in late October, with an average FPT of approximately 134 days. Maximum freezing depth (MFD) is generally reached in early to mid-March, followed by an MPT of approximately 59 days, ending around mid-May, yielding a mean annual FDT of approximately 192 days (Table 2).

Table 2. Statistics of freeze-thaw indicators (2000–2021)

Indicator	FSD	FPT	MFD_day
Days	301.4±26.6	134.1±26.7	75.2±16.6
Indicator	TPD	TMD	FDT
Days	58.7±19.4	132.6±26.2	191.7±36.1

Freeze-thaw indicators of SFG on the QTP exhibit pronounced regional differentiation. Freezing generally initiates earlier in the western Plateau such as the Gangdise and Karakoram Mountains, while eastern regions experience a delayed onset

https://doi.org/10.5194/egusphere-2026-2202
Preprint. Discussion started: 27 May 2026

including parts of the Hengduan Mountains (Fig.5a). Spatial gradient of thawing end dates is opposite, with earlier thawing occurring in the southeastern regions (Fig.5b). Both the FDT and MFD show high spatial consistency, with long-lasting frozen layers primarily distributed in the central and western cold regions (Fig.5b, c).

The spatial pattern of the freeze-thaw process reflects the combined influences of climatic gradients, topography, and surface energy balance. In high-altitude areas, low temperature and radiation deficit dominate the persistence of freezing, whereas in low-altitude regions, abundant heat input and weak snow cover lead to earlier thawing and shorter freezing periods.

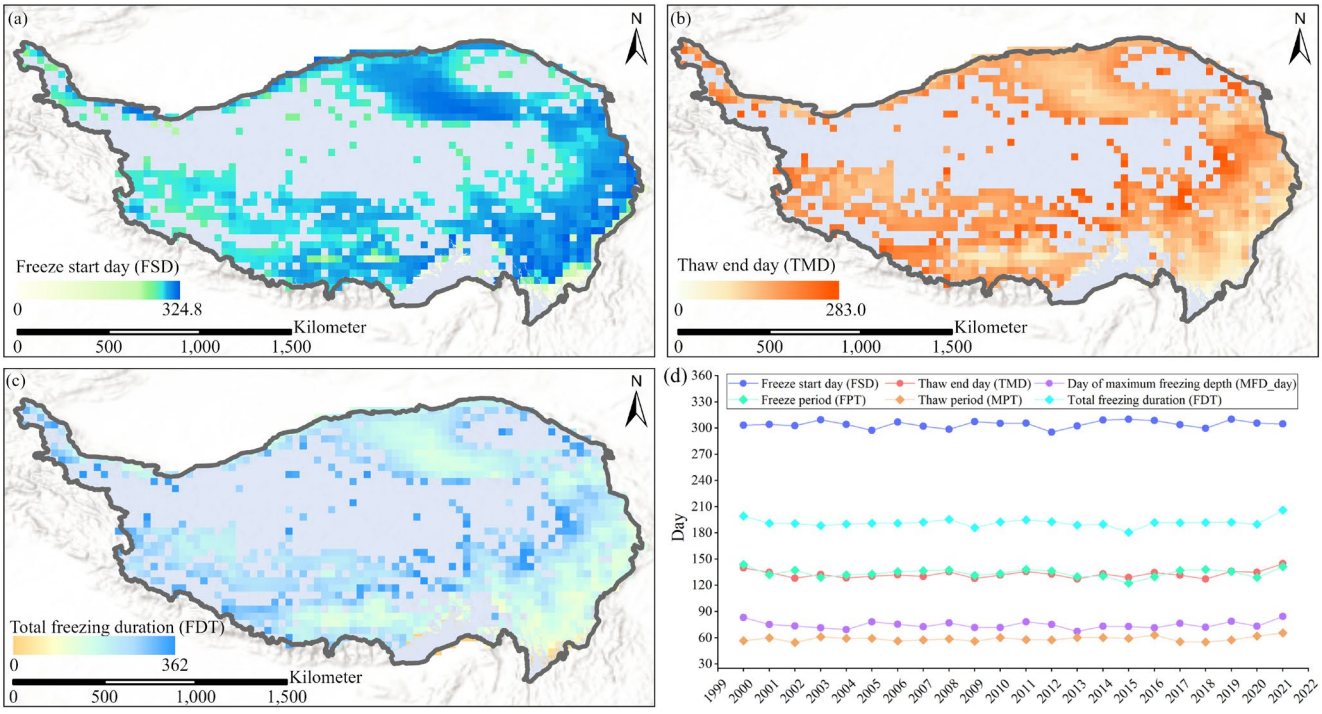

Figure 5: Spatial distribution and temporal variations of freeze-thaw process on the Qinghai-Tibet Plateau (2000-2021)

3.3 Model uncertainty and validation

To assess the influence of input data uncertainty, model structural assumptions, and scale-related differences on the estimation of lagged effects of extreme heat events, uncertainty analyses were conducted from three aspects: data perturbation, model robustness, and regional applicability of the methods.

At the data level, freezing depth was derived from interpolated multi-layer soil temperature profiles and thus inevitably contains uncertainties. To assess the sensitivity of lag-time estimates, two perturbation schemes were designed, including difference perturbations (±5, ±10, ±15, and ±20 cm) and proportional perturbations (±0.01, ±0.02, and ±0.05) (Ryan et al., 2018). The results show that the correlation coefficients between perturbed and original lag times all exceed 0.80 (with averages of 0.94 for difference perturbations and 0.85 for proportional perturbations), and all pass significance tests. This

https://doi.org/10.5194/egusphere-2026-2202
Preprint. Discussion started: 27 May 2026

indicates that uncertainties in freezing depth do not substantially alter the spatial patterns or relative magnitudes of the lagged response.

At the model level, the performance of the DLNM was evaluated using residual diagnostics, including Q-Q plots, residual distributions, and observed–fitted comparisons (Gasparrini et al., 2017). As shown in Fig.6, the Q-Q plot (Fig. 6a) indicates that model residuals are approximately normally distributed, although slight deviations occur at the tails, suggesting moderate uncertainty under extreme conditions. The residual-versus-linear-predictor relationship (Fig. 6b) shows no pronounced systematic structure across most prediction ranges, while residual variability increases when the linear predictor becomes large, indicating increased uncertainty at greater freezing depths. The residual histogram (Fig. 6c) further demonstrates that residuals are centered near zero with an approximately symmetric distribution. In addition, the comparison between residuals and fitted values (Fig. 6d) suggests that model errors remain relatively stable across most fitted ranges, although uncertainty slightly increases near the upper limit of freezing depth (approximately 2.5 m). Overall, these diagnostic results indicate that the DLNM adequately captures the lag-response structure of SFG to extreme heat events, while retaining acceptable robustness for regional-scale lag analysis.

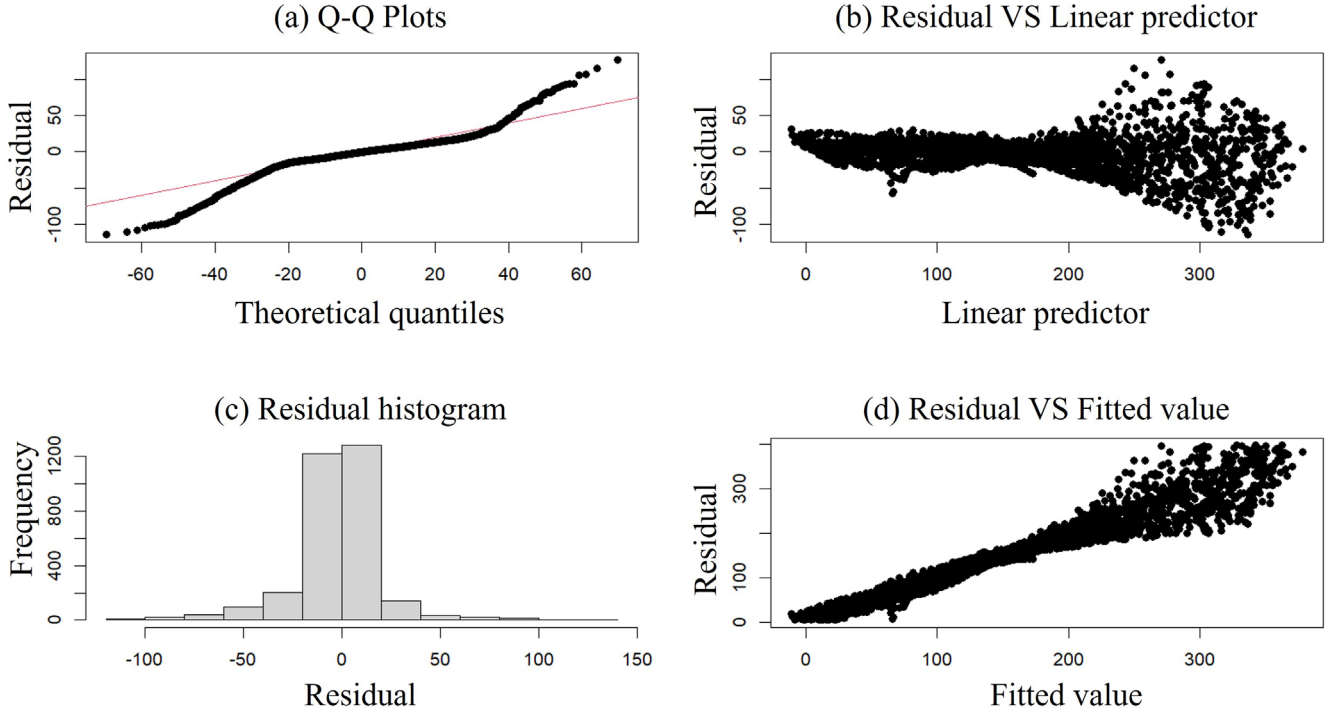

Figure 6: Uncertainty and diagnostic analysis results of the DLNM model

Regarding regional applicability, the use of pixel-scale data limits the ability to resolve local influences such as topography, snow cover, and vegetation heterogeneity on soil thermal processes (Ye et al., 2025), which may introduce biases in complex

https://doi.org/10.5194/egusphere-2026-2202
Preprint. Discussion started: 27 May 2026

terrain. Nevertheless, regional-scale analysis remains effective in capturing the dominant spatial patterns of lag effects (Gao et al., 2021).

Overall, the results from multiple perturbation experiments and model diagnostics demonstrate that the identified lagged responses of SFG are robust. The observed spatial heterogeneity is primarily driven by extreme heat forcing and soil hydrothermal processes, rather than by input uncertainties or model perturbations.

3.4 Lagged response characteristics of freezing depth to extreme heat events

This study examines extreme heat events and quantifies the magnitude and spatial variability of changes in freeze-thaw indicators under extreme heat conditions using anomaly-based analysis, in which response magnitudes are calculated as the differences between indicators under non-extreme-heat and extreme-heat conditions. When extreme heat events occur within one month prior to the TMD or FSD, the TMD is advanced by an average of 3.28 days, whereas the FSD is delayed by approximately 1.14 days. Substantial temporal variability exists (±10.18 and ±24.8 days, respectively). Moreover, the magnitude of these timing shifts scales with the duration of extreme heat: each additional extreme heat day advances the TMD by roughly 3.02 days and delays the FSD by about 1.52 days (Fig.7a, b), indicating that extreme heat accelerates the thawing process more strongly than it suppresses freezing initiation.

Ground-based observations further confirm that the MFD during months affected by extreme heat events is consistently shallower than during non-heat months (Fig.7c). MFD's reduction correlates closely with the number of heat days: each additional extreme heat day reduces MFD by approximately 1.12 cm on average (Fig.7d). These findings collectively demonstrate that extreme heat accelerates the shallowing of the seasonal frozen layer, disrupts thermal stability, and amplifies the sensitivity of the Plateau's permafrost environment to short-term thermal perturbations.

The observed shifts in FSD, TMD, and FPT suggest that short-duration extreme heat events can alter seasonal freeze-thaw dynamics in addition to long-term climatic warming. And the differences in lag responses among regions further indicate that local hydrothermal conditions, such as snow cover, soil moisture, and surface energy exchange, regulate the persistence of thermal disturbances in frozen soils. These findings highlight the importance of considering lagged thermal adjustments when interpreting frozen-ground dynamics and representing freeze-thaw processes under increasing climate extremes.

https://doi.org/10.5194/egusphere-2026-2202
Preprint. Discussion started: 27 May 2026

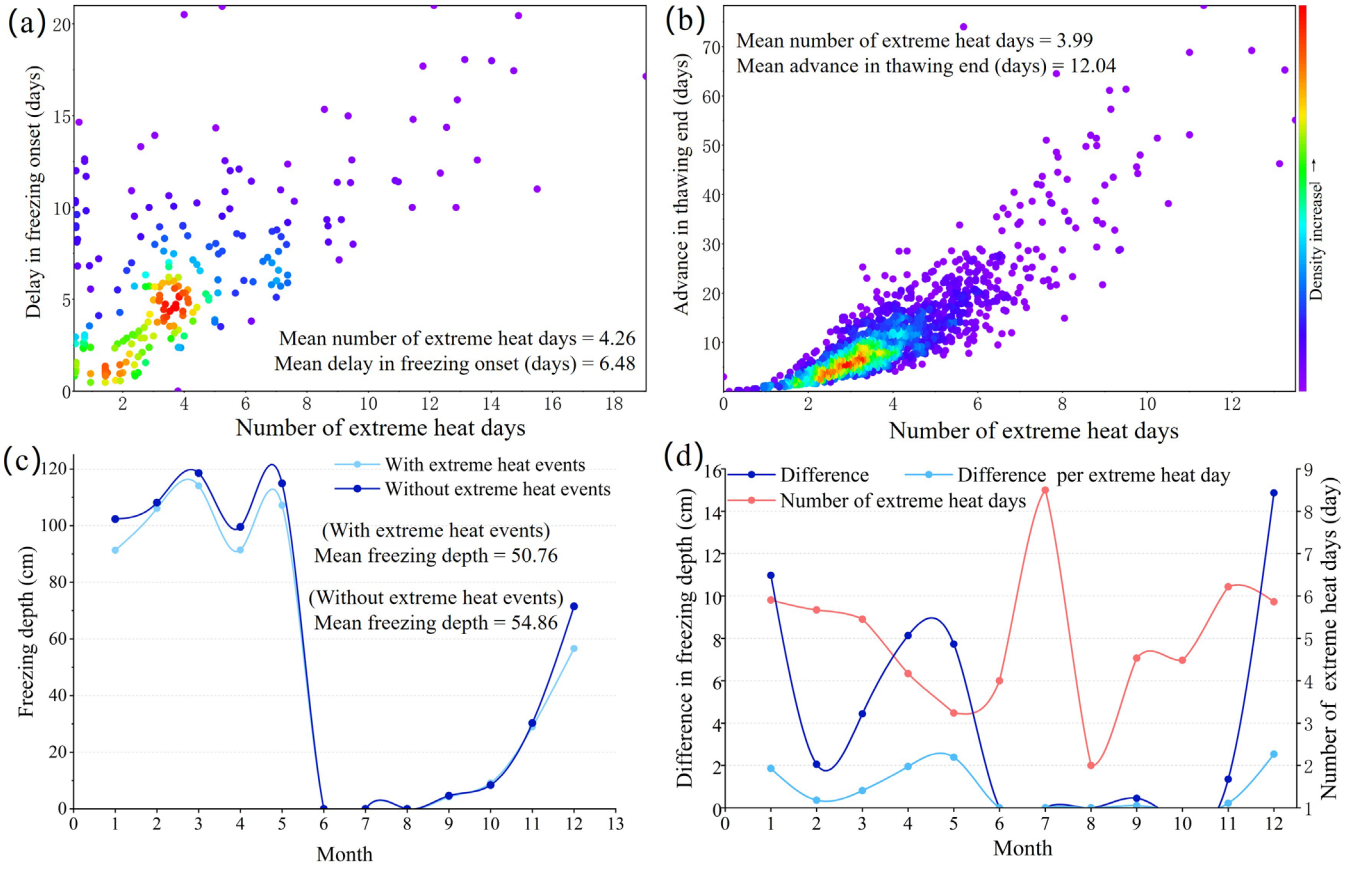

335 **Figure 7: Response of the freeze-thaw process of seasonally frozen ground to extreme heat events on the Qinghai-Tibet Plateau**

In addition, after accounting for hydrothermal covariates, extreme heat remained significantly associated with reduced freezing depth. This study explicitly characterizes a three-stage response pattern of SFG, comprising a rapid initiation phase, a delayed peak response, and a gradual recovery phase. On the one hand, the frozen-ground system exhibits both cumulative response and recovery capacity under short-term thermal perturbations. Freezing depth begins to show a noticeable response
340 within 5-10 days after the occurrence of extreme heat, reaches its maximum lagged effect around 15-25 days, and then gradually weakens and stabilizes (Fig.8). On the other hand, intense heat extremes trigger stronger and more localized perturbations in the shallow frozen layer, with a pronounced intensity dependence: higher-intensity events are associated with greater reductions in freezing depth and earlier peak responses. By comparison, moderate heat events produce more spatially diffuse but slower responses, characterized by delayed peaks and prolonged durations.

https://doi.org/10.5194/egusphere-2026-2202
Preprint. Discussion started: 27 May 2026

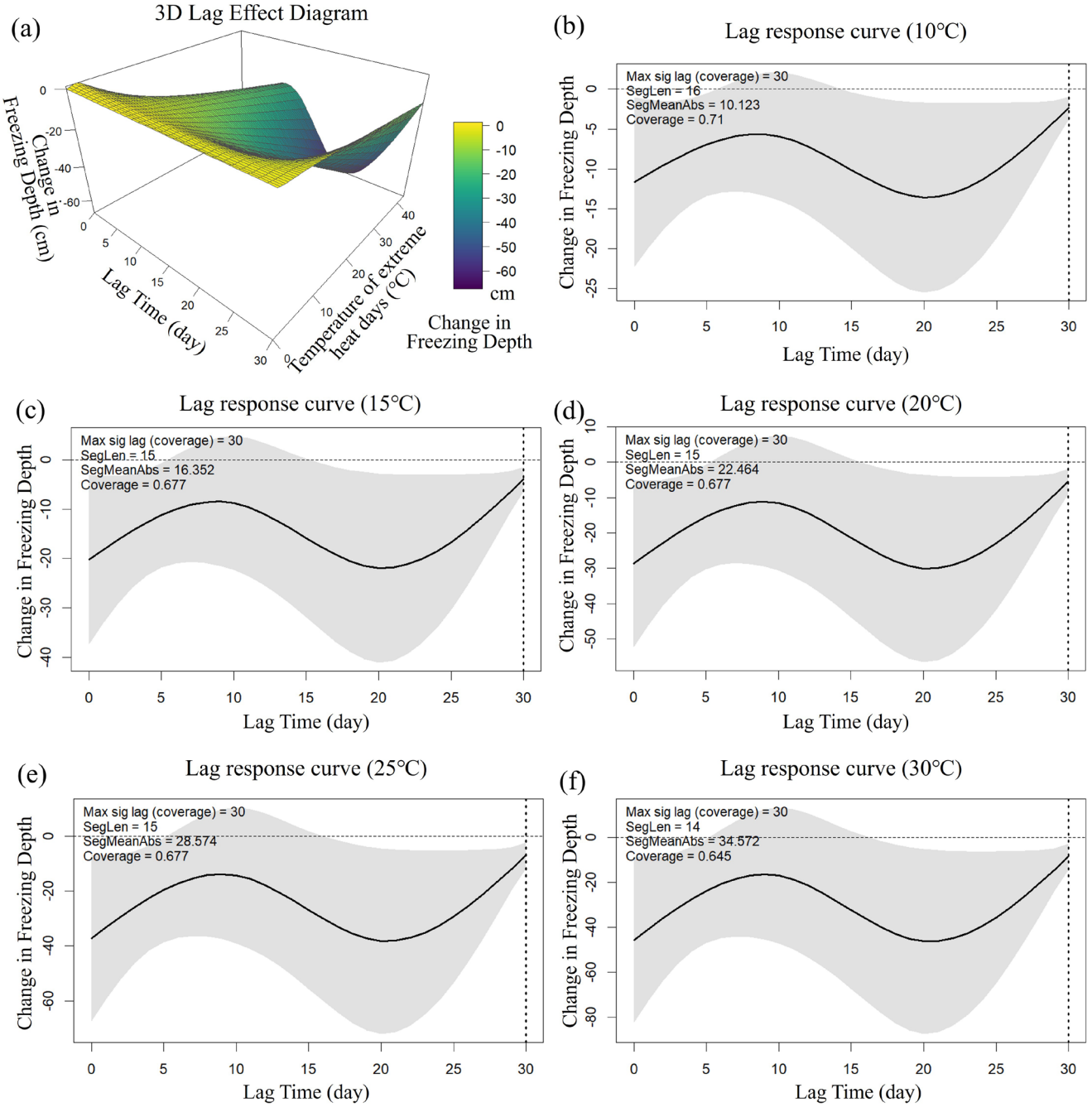

345

Figure 8: Lagged response of freezing depth in seasonally frozen ground to extreme heat events on the Qinghai-Tibet Plateau: (a) Three-dimensional lag-response surface between freezing-depth change, lag time, and temperature of extreme heat days; (b-f) Lag-response curves of freezing depth under representative extreme heat temperatures (10 °C, 15 °C, 20 °C, 25 °C, and 30 °C, respectively)

https://doi.org/10.5194/egusphere-2026-2202
Preprint. Discussion started: 27 May 2026

These lagged responses suggest that SFG responses to extreme heat are not instantaneous, but exhibit delayed thermal adjustments over subsequent days to weeks. This finding highlights the importance of subsurface heat storage and gradual energy redistribution in regulating freeze-thaw dynamics under short-term thermal disturbances.

4 Discussion

4.1 Physical basis of lagged thermal responses

Studies in the QTP and other high-latitude SFG regions show that heatwaves and extreme heat events alter freeze-thaw processes by enhancing surface energy fluxes, regulating soil moisture, and modifying snow cover conditions, which ultimately delay FSD, advance TMD, and shorten FPT (Chen et al., 2023; Chen et al., 2025). Since 2000, the freezing duration of SFG on the QTP has significantly shortened, and in years with frequent extreme heat events, heatwaves contribute approximately 6.6%-13.6% to seasonal thaw depth (Zhu et al., 2024). These findings suggest that the impacts of extreme heat on SFG are not instantaneous but involve delayed adjustments in subsurface thermal conditions (Dong et al., 2021).

The lagged response of SFG primarily originates from the thermal inertia of frozen soils and the relatively slow propagation of heat within the soil profile. Extreme heat events first alter near-surface thermal conditions and surface energy partitioning, after which heat propagates downward through soil thermal conduction (Li et al., 2021). Because subsurface soils require time to absorb, store, and redistribute thermal energy, the response of freezing processes often lags behind atmospheric warming. In particular, latent heat consumption during soil ice phase transitions requires substantial energy input for melting rather than temperature increase, thereby buffering rapid temperature changes and delaying thermal responses in the frozen layer (Tubini et al., 2021).

Compared with permafrost regions in the Arctic and other high latitudes, where lag times are typically 10-20 days (Batir et al., 2017), SFG on the QTP generally exhibits longer lagged responses exceeding 20 days (Fig. 8). This difference is likely associated with the Plateau's distinct continental and arid-cold climate, which shapes its hydrothermal conditions. The relatively high soil moisture variability and complex subsurface conditions on the QTP prolong heat transfer and enhance thermal storage within soils (Nitzbon et al., 2023). Together, these processes contribute to stronger thermal inertia and delayed responses of SFG to short-term thermal extremes.

Overall, the observed delay in freeze-thaw responses suggests that extreme heat events can influence frozen-ground dynamics beyond the timing of atmospheric forcing itself. Such delayed thermal adjustments imply that short-term climate extremes may contribute to seasonal frozen-ground variability in addition to long-term climatic warming, highlighting the importance of considering lag effects when interpreting freeze-thaw dynamics under increasing climate extremes.

https://doi.org/10.5194/egusphere-2026-2202
Preprint. Discussion started: 27 May 2026

4.2 Environmental controls on lagged responses

Although lagged responses to extreme heat are observed across the QTP, their magnitude and persistence vary considerably among regions (Fig.1, Fig.7a, b). Such regional differences are primarily associated with variations in hydrothermal conditions, surface energy exchange, and topographic environments, which jointly regulate subsurface heat storage and transfer processes (Chang et al., 2024; Harp et al., 2016).

The DLNM-XAI results indicate that the most influential factors include the duration of extreme heat events, snow depth, soil moisture, latent heat flux, and sensible heat flux (Fig.9a). Contrary to the conventional expectation that more intense or prolonged heat events tend to induce longer lagged responses (Decharme et al., 2013), lag time exhibits a negative relationship with the duration of extreme heat events and mean temperature exhibits a nonlinear response characterized by "amplification under moderate warming and attenuation under extreme heat" (Fig.9b, g). This behavior is likely associated with the thermal saturation mechanism of SFG (Gouttevin et al., 2012): moderate warming tends to enhance land–atmosphere thermal gradients and prolong lagged responses, whereas excessively strong warming may promote more rapid subsurface thermal adjustment, leading to shorter lag duration.

Snow cover exerts an important control through its combined insulation and radiative effects (Paquin and Sushama, 2015). Thick snow layers reduce conductive heat transfer between the atmosphere and soil while increasing surface albedo, thereby weakening effective ground heating and prolonging thermal adjustment processes (Damseaux et al., 2025; Pongracz et al., 2021). This mechanism is broadly consistent with the occurrence of longer lag durations in snow-rich and high-altitude areas of the Plateau.

Soil moisture influences lag duration through competing thermal mechanisms (Fig. 9c). Under relatively dry conditions, low thermal conductivity limits downward heat transfer and traps thermal energy near the surface, delaying subsurface responses. As soil moisture increases, enhanced thermal conductivity promotes heat propagation into deeper soil layers. At the same time, greater latent heat exchange associated with soil freeze-thaw transitions increases energy storage through phase-change processes, which may further extend lag duration (González-Rouco et al., 2021; Shirazi et al., 2009; Wang et al., 2025). These interactions suggest that the effect of soil moisture on lag duration is inherently nonlinear.

Meanwhile, the partitioning of surface energy fluxes further modulates the persistence of lagged responses (Fig.9d, f). Humid conditions generally enhance latent heat flux and accelerate energy dissipation through evaporation and phase-change processes, thereby reducing subsurface heat storage and shortening lag duration (Zhang and Sun, 2011). In contrast, dry and cold conditions suppress latent heat exchange and favor sensible heat accumulation, increasing heat retention near the surface and prolonging delayed thermal responses (Pradhan et al., 2019).

https://doi.org/10.5194/egusphere-2026-2202
Preprint. Discussion started: 27 May 2026

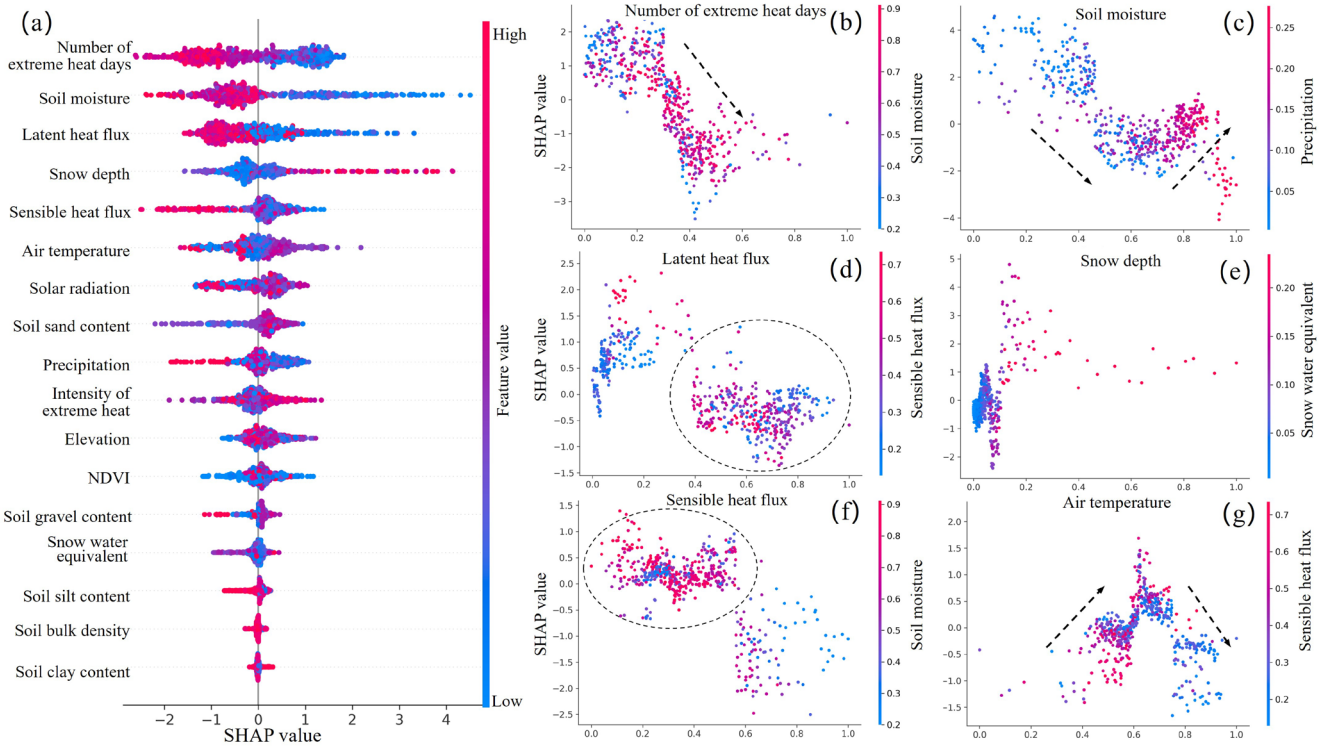

Figure 9: Dominant drivers of the maximum freezing-depth response to extreme heat on the Qinghai-Tibet Plateau: (a) Relative importance of environmental variables derived from SHAP values; (b-g) dependence relationships between lag duration and key environmental factors

Collectively, regional differences in lag duration are governed by coupled interactions among snow cover, soil hydrothermal conditions, surface energy exchange, and atmospheric forcing. For example, the Hengduan Mountains exhibit relatively long lag durations, potentially associated with rugged terrain, shaded slopes, deep valleys, and vegetation cover that reduce direct surface energy input (Hrbácek et al., 2021; Khan et al., 2021). Complex soil properties and high soil moisture may additionally enhance latent heat absorption and thermal buffering, contributing to prolonged thermal responses in this region (Beer et al., 2018). These findings indicate that the persistence of SFG responses to extreme heat depends not only on the intensity of thermal forcing but also on local environmental conditions, which regulate how thermal disturbances are stored, transferred, and dissipated within frozen soils.

4.3 Limitations and future perspectives

This study characterizes the lagged responses of SFG to extreme heat events over the QTP using multi-source data and a DLNM–XAI framework; however, several limitations remain.

First, the lag effect in SFG is fundamentally linked to soil ice content. Following surface heat input, energy is preferentially consumed by phase change rather than directly increasing soil temperature (Duan et al., 2025). Owing to the lack of reliable

https://doi.org/10.5194/egusphere-2026-2202
Preprint. Discussion started: 27 May 2026

large-scale observations of soil ice content, this study does not explicitly represent phase change processes or their regulatory effects on lagged responses, and instead relies on proxies such as soil moisture. This limits the mechanistic interpretation of the results. Future work should incorporate physically based freeze-thaw models or emerging data assimilation products to better quantify the role of latent heat in heat transfer.

Second, the active layer of permafrost also undergoes seasonal freeze-thaw cycles (Zhu et al., 2022), and its response to extreme climate events may share similarities with, but also differ from, that of SFG. Due to data constraints, this study does not systematically examine permafrost processes. Future research should extend the analysis across different frozen ground types (e.g., discontinuous permafrost, isolated patches, and sporadic permafrost) to enable comparative assessments in terms of permafrost extent and thermal structure.

Third, although the integration of multi-source datasets facilitates regional-scale analysis, the coupling of data with heterogeneous spatial resolutions may introduce uncertainties, particularly in regions with complex terrain or highly heterogeneous land surface conditions, potentially leading to under- or overestimation of lag effects. In addition, freezing depth is estimated from discretized soil temperature profiles using threshold-based methods, which may not accurately capture the true position of freeze-thaw interfaces (Cohen et al., 2021). Future studies should prioritize consistent-resolution datasets or apply scale-matching and downscaling approaches, together with improved interpolation methods, to enhance the accuracy of freezing depth estimation.

5 Conclusions

This study integrated observational data, multi-source remote sensing products, and reanalysis datasets with a baseline-based anomaly analysis and a DLNM-XAI framework to investigate the lagged responses of SFG to extreme heat events across the QTP. For the first time at the regional scale, the spatiotemporal heterogeneity and lagged response patterns of SFG to extreme heat events across the QTP are identified. The main conclusions are as follows:

(1) Extreme heat exerts significant impacts on the freeze-thaw dynamics of the QTP.

Extreme heat delays the freeze start day, advances the thaw end day, and accelerates the overall shallowing of freezing depth. Under extreme heat events, TMD was advanced by an average of 3.28 days, while FSD was delayed by 1.14 days. At the pixel/station scale, each additional day of extreme heat advanced TMD by 3.02 days, postponed FSD by 1.52 days, and reduced the freezing depth by 1.12 cm on average. These results demonstrate that extreme heat significantly disrupts the plateau's freeze-thaw rhythm and alters its surface–subsurface thermal equilibrium.

(2) The response of freezing depth to extreme heat exhibits a robust nonlinear lag structure with marked spatial differentiation.

At the regional-mean scale, the response of SFG on the QTP to extreme heat events typically follows a sequence of rapid onset (approximately 5-10 days), lag amplification (approximately 15-20 days), and gradual recovery. However, the duration of the lagged response varies substantially across regions. This spatial variability suggests that topographic and land surface

https://doi.org/10.5194/egusphere-2026-2202
Preprint. Discussion started: 27 May 2026

conditions may regulate surface energy balance and subsurface heat transfer, thereby shaping regionally differentiated lag characteristics in freezing depth responses.

(3) Lag duration is controlled by an integrated "soil condition-energy flux-climatic forcing" mechanism.

The timing and magnitude of lag effects are jointly determined by the duration of extreme heat events, snow depth, soil moisture, and surface energy fluxes. Long-duration heat events accelerate shallow-layer warming and thermal saturation, shortening lag times, whereas thick snow cover and higher soil moisture enhance latent heat buffering, prolonging lag responses. Sensible and latent heat fluxes interact with soil moisture and temperature to modulate energy dissipation, producing pronounced spatial heterogeneity. These soil thermal properties, energy transfer pathways, and atmospheric forcings jointly shape the heterogeneous lagged response characteristics of SFG to extreme heat events on the QTP.

Appendix A. Additional validation of freezing-depth estimation

To further evaluate the reliability of the interpolation-based freezing-depth estimates and respond to concerns regarding model bias, an additional comparison between observed and interpolated monthly maximum freezing depth was conducted using data from 69 stations during 2000-2015 (Fig. A1). The comparison shows a strong positive correlation (R = 0.77), indicating that the interpolation scheme effectively captures the temporal and spatial variability of freezing depth across the QTP. Although a systematic positive bias is evident (Bias = 39.79 cm), the deviations are mainly characterized by a relatively consistent offset rather than strong random dispersion. Given that this study primarily focuses on lag-response timing, spatial variability, and relative freeze-thaw dynamics, the interpolation results are considered sufficiently reliable for capturing large-scale trends in seasonal frozen-ground responses to extreme heat events.

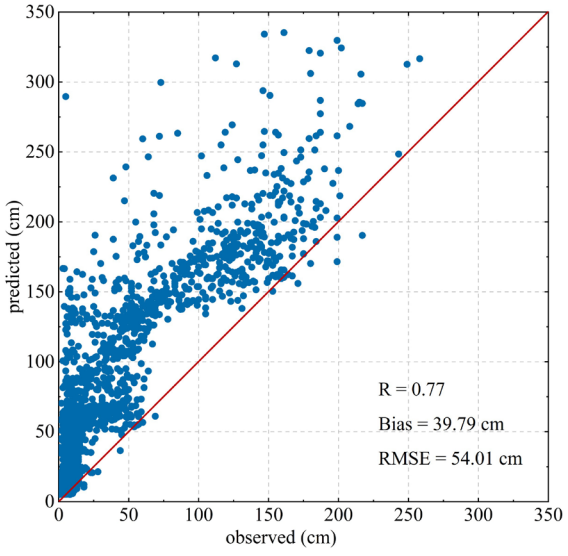

Figure A1. Scatter plot between observed and interpolated monthly maximum freezing depth across 69 stations during 2000-2015

https://doi.org/10.5194/egusphere-2026-2202
Preprint. Discussion started: 27 May 2026

Code and data availability

The datasets generated and analyzed during this study are publicly available in the Figshare repository at https://doi.org/10.6084/m9.figshare.32034888. The ERA5-Land data are available from the Copernicus Climate Data Store (https://cds.climate.copernicus.eu), and the CMA-RA/Land data can be obtained from the China Meteorological Administration. Other auxiliary datasets used in this study are publicly accessible from their respective providers as cited in the manuscript.

Author contributions

Ting Zhang designed the study, performed the analysis, and wrote the manuscript. Tingbin Zhang contributed to the study design and manuscript revision. Xianglong Ma contributed to manuscript editing and improvement. Guihua Yu provided funding support. Xianhang Zhou contributed to data collection. All authors contributed to the discussion of the results and approved the final manuscript.

Competing interests

The authors declare that they have no conflict of interest.

Acknowledgements

This work was supported by the Open Project of the Middle Yarlung Zangbo River Natural Resources Observation and Research Station (2024YJZKF002) and the General Program of the Sichuan Provincial Natural Science Foundation (2026NSFSC0137). The authors gratefully acknowledge the data providers for making their datasets publicly available, which made this study possible.

References

Bai, L., Cirendunzhu, Woodward, A., Dawa, Xiraoruodeng, and Liu, Q. Y.: Temperature and mortality on the roof of the world: A time-series analysis in three Tibetan counties, China, Science of the Total Environment, 485, 41-48, http://dx.doi.org/10.1016/j.scitotenv.2014.02.094, 2014.

Banerjee, A., Gupta, S., Priyanshu, P., Kar, A., Saha, R., Chakraborty, T., Ghosh, D., Kurths, J., and Hens, C.: Recent changes in spatiotemporal patterns of heat extremes in South Asia, Npj Climate and Atmospheric Science, 8, http://dx.doi.org/10.1038/s41612-025-01146-1, 2025.

https://doi.org/10.5194/egusphere-2026-2202
Preprint. Discussion started: 27 May 2026

Barriopedro, D., García-Herrera, R., Ordóñez, C., Miralles, D. G., and Salcedo-Sanz, S.: Heat Waves: Physical Understanding and Scientific Challenges, Reviews of Geophysics, 61, http://dx.doi.org/10.1029/2022rg000780, 2023.

Batir, J. F., Hornbach, M. J., and Blackwell, D. D.: Ten years of measurements and modeling of soil temperature changes and their effects on permafrost in Northwestern Alaska, Global and Planetary Change, 148, 55-71, http://dx.doi.org/10.1016/j.gloplacha.2016.11.009, 2017.

Beer, C., Porada, P., Ekici, A., and Brakebusch, M.: Effects of short-term variability of meteorological variables on soil temperature in permafrost regions, Cryosphere, 12, 741-757, http://dx.doi.org/10.5194/tc-12-741-2018, 2018.

Bibi, S., Wang, L., Li, X. P., Zhou, J., Chen, D. L., and Yao, T. D.: Climatic and associated cryospheric, biospheric, and hydrological changes on the Tibetan Plateau: a review, International Journal of Climatology, 38, E1-E17, http://dx.doi.org/10.1002/joc.5411, 2018.

Brunner, L. and Voigt, A.: Pitfalls in diagnosing temperature extremes, Nature Communications, 15, http://dx.doi.org/10.1038/s41467-024-46349-x, 2024.

Chang, T., Yi, Y. H., Jiang, H. R., Li, R. X., Lu, P., Liu, L., Wang, L. X., Zhao, L., Zwieback, S., and Zhao, J. Y.: Unraveling the non-linear relationship between seasonal deformation and permafrost active layer thickness, Npj Climate and Atmospheric Science, 7, http://dx.doi.org/10.1038/s41612-024-00866-0, 2024.

Chen, W. F., Yao, T. D., Zhang, G. Q., Woolway, R. I., Yang, W., Xu, F. L., and Zhou, T.: Glacier Surface Heatwaves Over the Tibetan Plateau, Geophysical Research Letters, 50, http://dx.doi.org/10.1029/2022gl101115, 2023.

Chen, Y. H., Guo, D. L., Wang, H. J., and Wang, A. H.: Observed Changes in Seasonal Surface Soil Freeze-Thaw Cycles in China and Subregions From 1981 to 2017 and Their Relationships With Meteorological Elements, Journal of Geophysical Research-Atmospheres, 130, http://dx.doi.org/10.1029/2024jd042351, 2025.

Chymyrov, A.: Comparison of different DEMs for hydrological studies in the mountainous areas, The Egyptian Journal of Remote Sensing and Space Science, 24, 587-594, http://dx.doi.org//10.1016/j.ejrs.2021.08.001, 2021.

Cohen, J., Rautiainen, K., Lemmetyinen, J., Smolander, T., Vehviläinen, J., and Pulliainen, J.: Sentinel-1 based soil freeze/thaw estimation in boreal forest environments, Remote Sensing of Environment, Vol.254, 112267, http://dx.doi.org/10.1016/j.rse.2020.112267, 2021.

Damseaux, A., Matthes, H., Dutch, V. R., Wake, L., and Rutter, N.: Impact of snow thermal conductivity schemes on pan-Arctic permafrost dynamics in the Community Land Model version 5.0, Cryosphere, 19, 1539-1558, http://dx.doi.org/10.5194/tc-19-1539-2025, 2025.

Decharme, B., Martin, E., and Faroux, S.: Reconciling soil thermal and hydrological lower boundary conditions in land surface models, Journal of Geophysical Research-Atmospheres, 118, 7819-7834, http://dx.doi.org/10.1002/jgrd.50631, 2013.

Di Napoli, C., Pappenberger, F., and Cloke, H. L.: Verification of Heat Stress Thresholds for a Health-Based Heat-Wave Definition, Journal of Applied Meteorology and Climatology, 58, 1177-1194, http://dx.doi.org/10.1175/jamc-d-18-0246.1, 2019.

https://doi.org/10.5194/egusphere-2026-2202
Preprint. Discussion started: 27 May 2026

Dong, X. F., Liu, C., Li, M., Ma, D. L., Chen, Q., and Zang, S. Y.: Variations in active layer soil hydrothermal dynamics of typical wetlands in permafrost region in the Great Hing'an Mountains, northeast China, Ecological Indicators, 129, http://dx.doi.org/10.1016/j.ecolind.2021.107880, 2021.

Duan, F., Quan, L., Wang, H., and Tian, B.: Effects of Cyclical Climate Change on Water Temperature Characteristics of Permafrost Slopes, Applied Sciences, 15, 3403, http://dx.doi.org/10.3390/app15063403, 2025.

Frauenfeld, O. W. and Zhang, T. J.: An observational 71-year history of seasonally frozen ground changes in the Eurasian high latitudes, Environmental Research Letters, 6, http://dx.doi.org/10.1088/1748-9326/6/4/044024, 2011.

Friedman, J. H.: Greedy function approximation: A gradient boosting machine, Annals of Statistics, 29, 1189-1232, http://dx.doi.org/10.1214/aos/1013203451, 2001.

Gao, T. G., Zhang, Y. L., Kang, S. C., Abbott, B. W., Wang, X. M., Zhang, T. J., Yi, S. H., and Gustafsson, O.: Accelerating permafrost collapse on the eastern Tibetan Plateau, Environmental Research Letters, 16, http://dx.doi.org/10.1088/1748-9326/abf7f0, 2021.

Gasparrini, A.: Modeling exposure-lag-response associations with distributed lag non-linear models, Statistics in Medicine, 33, 881-899, http://dx.doi.org/10.1002/sim.5963, 2014.

Gasparrini, A. and Armstrong, B.: Reducing and meta-analysing estimates from distributed lag non-linear models, Bmc Medical Research Methodology, 13, http://dx.doi.org/10.1186/1471-2288-13-1, 2013.

Gasparrini, A., Scheipl, F., Armstrong, B., and Kenward, M. G.: A Penalized Framework for Distributed Lag Non-Linear Models, Biometrics, 73, 938-948, http://dx.doi.org/10.1111/biom.12645, 2017.

González-Rouco, J. F., Steinert, N. J., García-Bustamante, E., Hagemann, S., De Vrese, P., Jungclaus, J. H., Lorenz, S. J., Melo-Aguilar, C., García-Pereira, F., and Navarro, J.: Increasing the Depth of a Land Surface Model. Part I: Impacts on the Subsurface Thermal Regime and Energy Storage, Journal of Hydrometeorology, 22, 3211-3230, http://dx.doi.org/10.1175/jhm-d-21-0024.1, 2021.

Gouttevin, I., Krinner, G., Ciais, P., Polcher, J., and Legout, C.: Multi-scale validation of a new soil freezing scheme for a land-surface model with physically-based hydrology, Cryosphere, 6, 407-430, http://dx.doi.org/10.5194/tc-6-407-2012, 2012.

Hajihosseinlou, M., Maghsoudi, A., and Ghezelbash, R.: A Novel Scheme for Mapping of MVT-Type Pb-Zn Prospectivity: LightGBM, a Highly Efficient Gradient Boosting Decision Tree Machine Learning Algorithm, Natural Resources Research, 32, 2417-2438, http://dx.doi.org/10.1007/s11053-023-10249-6, 2023.

Harp, D. R., Atchley, A. L., Painter, S. L., Coon, E. T., Wilson, C. J., Romanovsky, V. E., and Rowland, J. C.: Effect of soil property uncertainties on permafrost thaw projections: a calibration-constrained analysis, Cryosphere, 10, 341-358, http://dx.doi.org/10.5194/tc-10-341-2016, 2016.

Horton, R. M., Mankin, J. S., Lesk, C., Coffel, E., and Raymond, C.: A Review of Recent Advances in Research on Extreme Heat Events, Current Climate Change Reports, 2, 242-259, http://dx.doi.org/10.1007/s40641-016-0042-x, 2016.

https://doi.org/10.5194/egusphere-2026-2202
Preprint. Discussion started: 27 May 2026

Hrbácek, F., Engel, Z., Knazková, M., and Smolíková, J.: Effect of summer snow cover on the active layer thermal regime and thickness on CALM-S JGM site, James Ross Island, eastern Antarctic Peninsula, Catena, 207, http://dx.doi.org/10.1016/j.catena.2021.105608, 2021.

Ji, F., Shi, J., Yuan, S., Li, Z., Fan, L., Jin, J., Zhu, L., Yao, Y., and Zheng, C.: Holistic assessment of seasonally frozen ground changes on the Qinghai-Tibet Plateau, Journal of Hydrology, 666, http://dx.doi.org/10.1016/j.jhydrol.2025.134791, 2026.

Ji, Z. M. and Kang, S. C.: Evaluation of extreme climate events using a regional climate model for China, International Journal of Climatology, 35, 888-902, http://dx.doi.org/10.1002/joc.4024, 2015.

Kang, S. C., Xu, Y. W., You, Q. L., Flügel, W. A., Pepin, N., and Yao, T. D.: Review of climate and cryospheric change in the Tibetan Plateau, Environmental Research Letters, 5, http://dx.doi.org/10.1088/1748-9326/5/1/015101, 2010.

Ke, G., Meng, Q., Finley, T., Wang, T., Chen, W., Ma, W. D., Ye, Q. W., and Liu, T. Y.: LightGBM: a highly efficient gradient boosting decision tree, Advances in Neural Information Processing Systems, 302017.

Khan, M. A. R., Singh, S., Pandey, P., Bhardwaj, A., Ali, S. N., Chaturvedi, V., and Ray, P. K. C.: Modelling Permafrost Distribution in Western Himalaya Using Remote Sensing and Field Observations, Remote Sensing, 13, http://dx.doi.org/10.3390/rs13214403, 2021.

Li, H., Pan, X. D., Peng, X. Q., Washakh, R. M. A., Zheng, M., and Nie, X. W.: Projected changes in soil freeze depth and their eco-hydrological impacts over the Tibetan Plateau during the 21st century, Science of the Total Environment, 905, http://dx.doi.org/10.1016/j.scitotenv.2023.167074, 2023.

Li, Q., Xue, Y. K., and Liu, Y.: Impact of frozen soil processes on soil thermal characteristics at seasonal to decadal scales over the Tibetan Plateau and North China, Hydrology and Earth System Sciences, 25, 2089-2107, http://dx.doi.org/10.5194/hess-25-2089-2021, 2021.

Li, X. F., Zhao, L., Wang, S., Cheng, X. H., and Wang, L. X.: Unstable permafrost regions experience more severe heatwaves in a warming climate, Npj Climate and Atmospheric Science, 8, http://dx.doi.org/10.1038/s41612-025-01037-5, 2025.

Liu, S., Cheng, F., Dong, S., Zhao, H., Hou, X., and Wu, X.: Spatiotemporal dynamics of grassland aboveground biomass on the Qinghai-Tibet Plateau based on validated MODIS NDVI, Scientific Reports, 7, 4812, http://dx.doi.org/10.1038/s41598-017-04038-4, 2017.

Liu, Z., Jiang, L., Shi, C., Zhang, T., Zhou, Z., Liao, J., Yao, S., Liu, J., Wang, M., Wang, H., Liang, X., Zhang, Z., Yao, Y., Zhu, T., Chen, Z., Xu, W., Cao, L., Jiang, H., and Hu, K.: CRA-40/Atmosphere—The First-Generation Chinese Atmospheric Reanalysis (1979–2018): System Description and Performance Evaluation, Journal of Meteorological Research 37, 1-19, http://dx.doi.org/10.1007/s13351-023-2086-x, 2023.

Luo, S. Q., Wang, J. Y., Pomeroy, J. W., and Lyu, S. H.: Freeze-Thaw Changes of Seasonally Frozen Ground on the Tibetan Plateau from 1960 to 2014, Journal of Climate, 33, 9427-9446, http://dx.doi.org/10.1175/jcli-d-19-0923.1, 2020.

https://doi.org/10.5194/egusphere-2026-2202
Preprint. Discussion started: 27 May 2026

Ma, J. J., Li, R., Liu, H. C., Huang, Z. W., Wu, T. H., Hu, G. J., Xiao, Y., Zhao, L., Du, Y. Z., and Yang, S. H.: The Surface Energy Budget and Its Impact on the Freeze-thaw Processes of Active Layer in Permafrost Regions of the Qinghai-Tibetan Plateau, Advances in Atmospheric Sciences, 39, 189-200, http://dx.doi.org/10.1007/s00376-021-1066-2, 2022.

Mi, J. X., Li, A. D., and Zhou, L. F.: Review Study of Interpretation Methods for Future Interpretable Machine Learning, Ieee Access, 8, 191969-191985, http://dx.doi.org/10.1109/access.2020.3032756, 2020.

Mihalakakou, G., Santamouris, M., Lewis, J. O., and Asimakopoulos, D. N.: On the application of the energy balance equation to predict ground temperature profiles, Solar Energy, 60, 181-190, http://dx.doi.org/10.1016/s0038-092x(97)00012-1, 1997.

Muñoz-Sabater, J., Dutra, E., Agustí-Panareda, A., Albergel, C., Arduini, G., Balsamo, G., Boussetta, S., Choulga, M., Harrigan, S., Hersbach, H., Martens, B., Miralles, D. G., Piles, M., Rodríguez-Fernández, N. J., Zsoter, E., Buontempo, C., and and Thépaut, J.-N.: ERA5-Land: a state-of-the-art global reanalysis dataset for land applications, Earth System Science Data, 13, 4349–4383, http://dx.doi.org//10.5194/essd-13-4349-2021, 2021., 2021.

Neophytou, A. M., Picciotto, S., Brown, D. M., Gallagher, L. E., Checkoway, H., Eisen, E. A., and Costello, S.: Exposure-Lag-Response in Longitudinal Studies: Application of Distributed-Lag Nonlinear Models in an Occupational Cohort, American Journal of Epidemiology, 187, 1539-1548, http://dx.doi.org/10.1093/aje/kwy019, 2018.

Nitzbon, J., Krinner, G., von Deimling, T. S., Werner, M., and Langer, M.: First Quantification of the Permafrost Heat Sink in the Earth's Climate System, Geophysical Research Letters, 50, http://dx.doi.org/10.1029/2022gl102053, 2023.

Paquin, J. P. and Sushama, L.: On the Arctic near-surface permafrost and climate sensitivities to soil and snow model formulations in climate models, Climate Dynamics, 44, 203-228, http://dx.doi.org/10.1007/s00382-014-2185-6, 2015.

Parker, L. E., McElrone, A. J., Ostoja, S. M., and Forrestel, E. J.: Extreme heat effects on perennial crops and strategies for sustaining future production, Plant Science, 295, http://dx.doi.org/10.1016/j.plantsci.2019.110397, 2020.

Pascual, D. and Johansson, M.: Increasing impacts of extreme winter warming events on permafrost, Weather and Climate Extremes, 36, http://dx.doi.org/10.1016/j.wace.2022.100450, 2022.

Pongracz, A., Wårlind, D., Miller, P. A., and Parmentier, F. J. W.: Model simulations of arctic biogeochemistry and permafrost extent are highly sensitive to the implemented snow scheme in LPJ-GUESS, Biogeosciences, 18, 5767-5787, http://dx.doi.org/10.5194/bg-18-5767-2021, 2021.

Pradhan, N. R., Downer, C. W., and Marchenko, S.: Catchment Hydrological Modeling with Soil Thermal Dynamics during Seasonal Freeze-Thaw Cycles, Water, 11, http://dx.doi.org/10.3390/w11010116, 2019.

Ran, Y., Li, X., Che, T., Wang, B., and Cheng, G.: Current state and past changes in frozen ground at the Third Pole. In: National Tibetan Plateau / Third Pole Environment Data Center, Center, N. T. P. T. P. E. D. (Ed.), http://dx/doi.org/18406.11.Cryos.tpdc.272790, 2022a.

Ran, Y. H., Li, X., Che, T., Wang, B. Q., and Cheng, G. D.: Current state and past changes in frozen ground at the Third Pole: A research synthesis, Advances in Climate Change Research, 13, 632-641, http://dx.doi.org/10.1016/j.accre.2022.09.004, 2022b.

https://doi.org/10.5194/egusphere-2026-2202
Preprint. Discussion started: 27 May 2026

Ryan, E., Wild, O., Voulgarakis, A., and Lee, L.: Fast sensitivity analysis methods for computationally expensive models with multi-dimensional output, Geoscientific Model Development, 11, 3131-3146, http://dx.doi.org/10.5194/gmd-11-3131-2018, 2018.

Shirazi, T., Allen, D. M., Quinton, W. L., and Pomeroy, J. W.: Estimating soil thaw energy in sub-Alpine tundra at the hillslope scale, Wolf Creek, Yukon Territory, Canada, Hydrology Research, 40, 1-18, http://dx.doi.org/10.2166/nh.2009.043, 2009.

Song, L., Wang, L., Zhou, J., Luo, D. L., and Li, X. P.: Divergent runoff impacts of permafrost and seasonally frozen ground at a large river basin of Tibetan Plateau during 1960-2019, Environmental Research Letters, 17, http://dx.doi.org/10.1088/1748-9326/aca4eb, 2022.

Staniec, M. and Nowak, H.: The application of energy balance at the bare soil surface to predict annual soil temperature distribution, Energy and Buildings, 127, 56-65, http://dx.doi.org/10.1016/j.enbuild.2016.05.047, 2016.

Stiegler, C., Johansson, M., Christensen, T. R., Mastepanov, M., and Lindroth, A.: Tundra permafrost thaw causes significant shifts in energy partitioning, Tellus Series B-Chemical and Physical Meteorology, 68, http://dx.doi.org/10.3402/tellusb.v68.30467, 2016.

Sulikowska, A. and Wypych, A.: Summer temperature extremes in Europe: how does the definition affect the results?, Theoretical and Applied Climatology, 141, 19-30, http://dx.doi.org/10.1007/s00704-020-03166-8, 2020.

Tao, J., Liljedahl, A. K., Burn, C. R., Grosse, G., Noetzli, J., Goetz, S. J., Douglas, T. A., and Yang, Y. H.: Permafrost vulnerability to climate change: understanding thaw dynamics and climate feedback of permafrost degradation, Environmental Research Letters, 20, http://dx.doi.org/10.1088/1748-9326/adfc7e, 2025.

Teskey, R., Wertin, T., Bauweraerts, I., Ameye, M., McGuire, M. A., and Steppe, K.: Responses of tree species to heat waves and extreme heat events, Plant Cell and Environment, 38, 1699-1712, http://dx.doi.org/10.1111/pce.12417, 2015.

Tubini, N., Gruber, S., and Rigon, R.: A method for solving heat transfer with phase change in ice or soil that allows for large time steps while guaranteeing energy conservation, Cryosphere, 15, 2541-2568, http://dx.doi.org/10.5194/tc-15-2541-2021, 2021.

Van den Broeck, G., Lykov, A., Schleich, M., and Suciu, D.: On the Tractability of SHAP Explanations, Journal of Artificial Intelligence Research, 74, 851-886, http://dx.doi.org/10.1613/jair.1.13283, 2022.

Van den Heuvel, E. and Zhan, Z. Z.: Myths About Linear and Monotonic Associations: Pearson's r, Spearman's ρ, and Kendall's τ, American Statistician, 76, 44-52, http://dx.doi.org/10.1080/00031305.2021.2004922, 2022.

Wang, Y. N., Wu, J. F., Zhang, J. Y., Guan, T. S., Wang, G. Q., Jin, J. L., and Wang, Z. L.: Depth distributions of soil temperature: Seasonal sensitivity and simulation across dryness/wetness conditions, Agricultural Water Management, 316, http://dx.doi.org/10.1016/j.agwat.2025.109571, 2025.

Wen, B., Zhang, T. B., Zhou, X. B., Yi, G. H., Li, J. J., Bie, X. J., and Chen, Y.: Variation characteristics of frozen ground degradation in the Qinghai-Tibet Plateau observed using time series data of MODIS from 2000 to 2020, Theoretical and Applied Climatology, 151, 1673-1686, http://dx.doi.org/10.1007/s00704-022-04344-6, 2023.

https://doi.org/10.5194/egusphere-2026-2202
Preprint. Discussion started: 27 May 2026

Xu, X. M., Zhang, Z. Q., Tai, B. W., Gao, S. R., Yang, Y. Z., and Wu, Q. B.: Climate warming and wetting poses a severe threat to permafrost engineering stability on the Qinghai-Xizang Plateau, Advances in Climate Change Research, 16, 93-108, http://dx.doi.org/10.1016/j.accre.2025.02.001, 2025.

Yao, J. M., Zhao, L., Gu, L. L., Qiao, Y. P., and Jiao, K. Q.: The surface energy budget in the permafrost region of the Tibetan Plateau, Atmospheric Research, 102, 394-407, http://dx.doi.org/10.1016/j.atmosres.2011.09.001, 2011.

Ye, K. H., Cohen, J., Chen, H. W., Zhang, S. Y., Luo, D. H., and Hamouda, M. E.: Attributing climate and weather extremes to Northern Hemisphere sea ice and terrestrial snow: progress, challenges and ways forward, Npj Climate and Atmospheric Science, 8, http://dx.doi.org/10.1038/s41612-025-01012-0, 2025.

Yu, Y., Shao, Q. X., Lin, Z. H., and Kang, I. S.: Characteristics Analysis and Synoptic Features of Event-Based Regional Heatwaves Over China, Journal of Geophysical Research-Atmospheres, 126, http://dx.doi.org/10.1029/2020jd033865, 2021.

Zhang, C., Qin, D. H., and Zhai, P. M.: Amplification of warming on the Tibetan Plateau, Advances in Climate Change Research, 14, 493-501, http://dx.doi.org/10.1016/j.accre.2023.07.004, 2023.

Zhang, X. and Sun, S. F.: The Impact of Soil Freezing/Thawing Processes on Water and Energy Balances, Advances in Atmospheric Sciences, 28, 169-177, http://dx.doi.org/10.1007/s00376-010-9206-0, 2011.

Zhao, Z. H., Fu, R. Y., Liu, J. J., Dai, L. C., Guo, X. W., Du, Y. G., Hu, Z. M., and Cao, G. M.: Response of Seasonally Frozen Ground to Climate Changes in the Northeastern Qinghai-Tibet Plateau, Frontiers in Environmental Science, 10, http://dx.doi.org/10.3389/fenvs.2022.912209, 2022.

Zhu, X., Wu, T., Ni, J., Wu, X., Hu, G., Wang, S., Li, X., Wen, A., Li, R., Shang, C., and Ma, X.: Increased extreme warming events and the differences in the observed hydrothermal responses of the active layer to these events in China's permafrost regions, Climate Dynamics, Vol.59, 785-804, http://dx.doi.org/10.1007/s00382-022-06155-x, 2022.

Zhu, X. F., Wu, T. H., Chen, J., Wu, X. D., Wang, P. L., Zou, D. F., Yue, G. Y., Yan, X. C., Ma, X., Wang, D., Lou, P. Q., Wen, A. M., Shang, C. P., and Liu, W. Y.: Summer heat wave in 2022 led to rapid warming of permafrost in the central Qinghai-Tibet Plateau, Npj Climate and Atmospheric Science, 7, http://dx.doi.org/10.1038/s41612-024-00765-4, 2024.